Unconditionally Stable D–H FDTD Formulation with Anisotropic PML Boundary Conditions

Gianluca Lazzi, *Senior Member, IEEE*

***Abstract*—An unconditionally stable finite difference time domain (FDTD) method based on a D–H formulation and the recently proposed alternating-direction-implicit (ADI) marching scheme is presented. The advantage of the D–H algorithm over the conventional E–H is the possibility to easily implement an unsplit field components formulation of the PML absorbing boundary condition that is independent from the background material used in the FDTD grid. The method allows therefore immersing any dielectric in the PML layers without any special consideration, and is amenable for models truncation often used in biomedical simulations. Furthermore, the proposed scheme can be extended to account for frequency dispersive dielectrics.**

***Index Terms*—ADI, FDTD methods, PML.**

I. Introduction

THE possibility of using the alternating-direction-implicit (ADI) scheme to produce an unconditionally stable finite difference time domain (FDTD) code has recently been proposed [1]–[5]. The method removes completely the conventional need to resort to time stepping resolution strictly related to the spatial resolution of the FDTD grid by means of the Courant stability condition. In particular, it has been shown in [3], [5] that the new ADI-FDTD is unconditionally stable, for any given time resolution Δt and, therefore, the choice of Δt is based only on the desired accuracy.

In this letter, the ADI-FDTD scheme is extended and applied to a D–H formulation with unsplit-field components PML boundary conditions [6]–[8]. The proposed formulation of the PML conditions differs from that in [9], which is based on the split-field formulation of Berenger. The proposed algorithm therefore combines the advantages presented by the algorithms in [2]–[5] and [6], in the sense that the PML condition is independent from the background material used in the FDTD grid (meaning that the PML conductivity profile is not a function of the dielectric properties of the material) and the Courant stability condition is removed. Even though not in its more general formulation given in [10], the method allows immersing any dielectric in the PML layers without any special consideration, and is therefore amenable for models truncation often used in biomedical simulations. Furthermore, the proposed scheme can be extended to account for frequency dispersive dielectrics.

Manuscript received October 19, 2000; revised January 17, 2001. The review of this letter was arranged by Associate Editor Dr. Ruediger Vahldieck.

The author is with the Department of Electrical and Computer Engineering, North Carolina State University, Raleigh, NC 27695 USA (e-mail: lazzi@eos.ncsu.edu).

Publisher Item Identifier S 1531-1309(01)03329-3.

II. D–H ADI FDTD Formulation

The equations to be used in the D–H ADI FDTD formulation with PML boundary conditions are given in [6]. For brevity, in the following we describe the algorithm as applied to one of the six equations. The normalized equation for D_x according to [6] is, for example

$$j\omega\left(1+\frac{\sigma_x^p(x)}{j\omega\varepsilon_0}\right)^{-1}\left(1+\frac{\sigma_y^p(y)}{j\omega\varepsilon_0}\right)\left(1+\frac{\sigma_z^p(z)}{j\omega\varepsilon_0}\right)D_x = c_0\left(\frac{\partial H_z}{\partial y}-\frac{\partial H_y}{\partial z}\right) \tag{1}$$

with σ_i^p conductivities of the PML layers in the x, y, and z directions. As in [2]–[5], the ADI-FDTD is implemented in two steps. Referring to (1), in the first half step H_z is computed at the same time on which D_x needs to be calculated, while in the second half step H_y is computed at the same time step on which D_x needs to be calculated. Following a procedure similar to that in [6], [7], the discretized form of (1) that one obtains is given by (2), shown at the bottom of the next page, for the first half-step, where the following notation has been used:

$$x_1(i)=\frac{2\varepsilon_0-\sigma_x^p(i)\Delta t}{2\varepsilon_0+\sigma_x^p(i)\Delta t} \tag{3}$$

$$x_2(i)=\frac{2\varepsilon_0}{2\varepsilon_0+\sigma_x^p(i)\Delta t} \tag{4}$$

$$x_3(i)=1+\frac{\sigma_x^p(i)\Delta t}{\varepsilon_0}. \tag{5}$$

Similar notation has been used for the y_is and z_is. To obtain from (2) a useful formula that relates D_x at time step $n+1/2$ to fields at the previous time step n, the expression of H_z at time step $n+1/2$ is necessary. By using the normalized equation

$$j\omega\left(1+\frac{\sigma_x(x)}{j\omega\varepsilon_0}\right)\left(1+\frac{\sigma_y(y)}{j\omega\varepsilon_0}\right)\left(1+\frac{\sigma_z(z)}{j\omega\varepsilon_0}\right)^{-1}H_z = c_0\left(\frac{\partial E_x}{\partial y}-\frac{\partial E_y}{\partial x}\right) \tag{6}$$

one can obtain the discretized expression of H_z at time step $n+1/2$ as a function of the electric field E_x computed at time step $n+1/2$ and E_y computed at time step n. This results in (7), shown at the bottom of the next page. Next, it should be noted that the E_x computed at time step $n+1/2$ in (7) can be expressed as a function of the D_x field at the same time step and the E_x field at previous time steps. For a nondispersive dielectric with relative dielectric constant ε_{rx} and conductivity σ_x in the x direction, this relation becomes

$$E_x^{n+1/2}\Big|_{i+1/2,\,j,\,k} = \frac{D_x^{n+1/2}\Big|_{i+1/2,\,j,\,k} - \frac{\sigma_x \Delta t}{\varepsilon_0}\sum_{s=1}^{2n} E_x^{s/2}\Big|_{i+1/2,\,j,\,k}}{\varepsilon_{rx} + \frac{\sigma_x \Delta t}{\varepsilon_0}}. \quad (8)$$

By substituting (8) into (7), and the resulting expression into (2), one finally obtains an equation that relates $D_x^{n+1/2}|_{i+1/2,\,j-1,\,k}$, $D_x^{n+1/2}|_{i+1/2,\,j,\,k}$, and $D_x^{n+1/2}|_{i+1/2,\,j+1,\,k}$ to D, E, H fields at time step n and the summation of the E and H fields components up to time step n. The final equation is not given here due to space limitation. This leads to a tridiagonal system of equation that can be easily solved. The second half time step for D_x can be derived similarly. Proceeding in analogous manner for the remaining two D field components completes the algorithm. It should be noted that, while the obtained equations appear to be considerably more complicated and computationally intensive than those reported in [2]–[5], most of the terms are 0 and many coefficients (such as the x_is, y_is, z_is) are identically 1 for non-PML regions. This means that the computer code to implement the proposed algorithm will exhibit only a slight additional load in the non-PML regions due to the additional calculation of the E field from the D field. However, while in non-PML regions the complexity of the resulting equations is very similar to that in [2]–[5], in the PML regions all the terms in the resulting equations need to be retained.

III. Results

A number of tests have been performed to verify the accuracy of the proposed algorithm. Since one of the main advantages of the algorithm is the possibility of defining dielectrics in the FDTD grid independently from the PML boundary conditions, a test case where half of the FDTD space is filled with a lossy dielectric has been considered. A $\lambda/8$ dipole at the frequency of 900 MHz is placed in front of a dielectric slab ($\varepsilon_r = 10$, $\sigma = 0.1$ S/m). The FDTD space is composed by $62 \times 52 \times 117$ cells in the x, y, and z directions, respectively, and the dielectric slab occupies half of the space in the x direction (and is therefore composed by $31 \times 52 \times 117$ cells). The grid resolution is 0.5 mm, and the dipole is placed at a distance of 2.5 mm from the slab, with its axis oriented in the z direction. Under these conditions,

$$\begin{aligned} D_x^{n+1/2}\Big|_{i+1/2,\,j,\,k} &= y_1(j)z_1(k)\, D_x^n\big|_{i+1/2,\,j,\,k} + c_0\Delta t y_2\left(j+\tfrac{1}{2}\right) z_2(k) x_3 \cdot \left(i+\frac{1}{2}\right) \\ &\left(\frac{H_z^{n+1/2}\Big|_{i+1/2,\,j+1/2,\,k} - H_z^{n+1/2}\Big|_{i+1/2,\,j-1/2,\,k}}{\Delta y}\right) \\ &- c_0\Delta t y_2\left(j+\frac{1}{2}\right) z_2(k)\cdot\left(\frac{H_y^n\big|_{i+1/2,\,j,\,k+1/2} - H_y^n\big|_{i+1/2,\,j,\,k-1/2}}{\Delta z}\right) + c_0\frac{\sigma_x^p\left(i+\frac{1}{2}\right)\Delta t^2}{\varepsilon_0} \\ &\cdot\left[\sum_{s=1}^{2n}\left(\frac{H_z^{s/2}\Big|_{i+1/2,\,j+1/2,\,k} - H_z^{s/2}\Big|_{i+1/2,\,j-1/2,\,k}}{\Delta y}\right) - \sum_{s=1}^{2n}\left(\frac{H_y^{s/2}\Big|_{i+1/2,\,j,\,k+1/2} - H_y^{s/2}\Big|_{i+1/2,\,j,\,k-1/2}}{\Delta z}\right)\right] \end{aligned} \quad (2)$$

$$\begin{aligned} H_z^{n+1/2}\Big|_{i+1/2,\,j+1/2,\,k} =& x_i\left(i+\tfrac{1}{2}\right) y_1\left(j+\tfrac{1}{2}\right) H_z^n\big|_{i+1/2,\,j+1/2,\,k} + c_0\Delta t x_2\cdot\left(i+\frac{1}{2}\right) \\ & y_2(j)z_3(k)\left(\frac{E_x^{n+1/2}\Big|_{i+1/2,\,j+1,\,k} - E_x^{n+1/2}\Big|_{i+1/2,\,j,\,k}}{\Delta y}\right) \\ & - c_0\Delta t\cdot x_2\left(i+\frac{1}{2}\right) y_2(j)\left(\frac{E_y^n\big|_{i+1,\,j+1/2,\,k} - E_y^n\big|_{i,\,j+1/2,\,k}}{\Delta x}\right) + c_0\frac{\sigma^p z(i+\frac{1}{2})\Delta t^2}{\varepsilon_0} \\ & \cdot\left[\sum_{s=1}^{2n}\left(\frac{E_x^{s/2}\Big|_{i+1/2,\,j+1,\,k} - E_x^{s/2}\Big|_{i+1/2,\,j,\,k}}{\Delta y}\right) - \sum_{s=1}^{2n}\left(\frac{E_y^{s/2}\Big|_{i+1,\,j+1/2,\,k} - E_y^{s/2}\Big|_{i,\,j+1/2,\,k}}{\Delta x}\right)\right] \end{aligned} \quad (7)$$

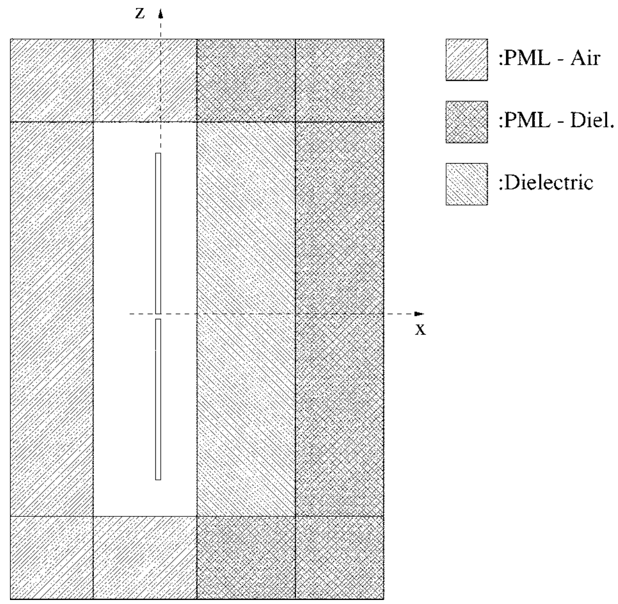

Fig. 1. Geometry of the considered test case. A $\lambda/8$ dipole is placed in front of a lossy dielectric slab ($\varepsilon_r = 10, \sigma = 0.1$ S/m), at a distance of 2.5 cm. Note that the lossy slab is immersed in the PML region to simulate an infinite slab.

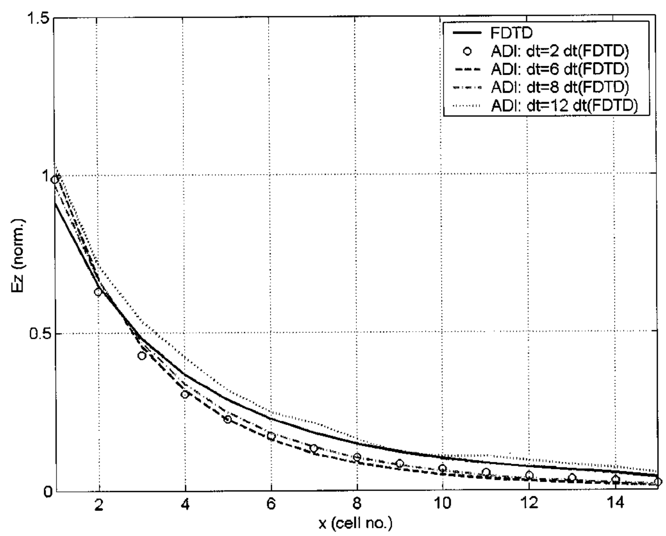

Fig. 2. Ez field in the slab along the x axis for various cases of D–H ADI FDTD and for the classical FDTD scheme.

the dipole extends from cell $26 \times 26 \times 21$ to cell $26 \times 26 \times 96$. The number of PML absorbing layers has been set to 16, and the conductivity profile has been selected similarly to [6].

Fig. 1 depicts the geometry for the considered test case, while Fig. 2 shows the profile of the normalized z directed E field inside the dielectric material along the x axis, at the y and z coordinates of the dipole feedpoint, calculated by using the classical FDTD and the D–H ADI-FDTD methods. Time steps Δt equal to two, six, eight, and 12 times the maximum Δt usable with the traditional FDTD method have been considered for the D–H ADI-FDTD. The agreement between the traditional FDTD and the proposed method is good, especially considering that the electric field values in the slab shown in Fig. 2 are approximately 100 times smaller than the highest value in the mesh for each of the considered cases.

IV. Conclusions and Final Remarks

The ADI-FDTD scheme is extended and applied to a D–H formulation with unsplit-field components PML boundary conditions. Results show that the method has the potential of solving with good accuracy realistic problems such as the interaction of a dipole with an infinite lossy dielectric slab. The advantages of the method are the following:

1) it remains stable beyond the Courant stability limit of the classical FDTD scheme;
2) the PML boundary condition is independent from the background material used in the FDTD grid;
3) it can be extended to account for frequency dependent dielectrics by simply modifying equation (8) in the derivation of the method.

The method can be efficiently coded, even though it requires a slightly longer execution time per time step than the regular FDTD code. Similarly to the conclusions reported in [9], it has been observed that the PML performance tends to degrade with increasing Δt, and a more detailed investigation is necessary to understand the performance variation of the PML layers with the conductivity profile for the D–H ADI FDTD method.

References

[1] T. Namiki, "A new FDTD algorithm based on alternating-direction implicit method," *IEEE Trans. Microwave Theory Tech.*, vol. 47, pp. 2003–2007, Oct. 1999.
[2] F. Zheng, Z. Chen, and J. Zhang, "A finite-difference time-domain method without the courant stability condition," *IEEE Microwave Guided Wave Lett.*, vol. 9, pp. 441–443, Nov. 1999.
[3] ——, "Toward the development of a three-dimensional unconditionally stable finite-difference time-domain method," *IEEE Trans. Microwave Theory Tech.*, vol. 48, pp. 1550–1558, Sept. 2000.
[4] T. Namiki, "3-D ADI FDTD method—Unconditionally stable time-domain algorithm for solving full vector Maxwell's equations," *IEEE Trans. Microwave Theory Tech.*, vol. 48, pp. 1743–1748, Oct. 2000.
[5] A. Taflove and S. C. Hagness, *Computational Electrodynamics: The Finite-Difference Time-Domain Method*, 2nd ed. Boston, MA: Artech, 2000.
[6] D. Sullivan, "An unsplit step 3-D PML for use with the FDTD method," *IEEE Microwave Guided Wave Lett.*, vol. 7, pp. 184–186, July 1997.
[7] D. Sullivan, *Electromagnetic Simulation Using the FDTD Method*. New York: IEEE Press, 2000.
[8] G. Lazzi, O. P. Gandhi, and D. Sullivan, "Use of PML absorbing layers for the truncation of the head model in cellular telephone simulations," *IEEE Trans. Microwave Theory Tech.*, Nov. 2000.
[9] G. Liu and S. C. Gedney, "Perfectly matched Laler for an unconditionally stable three-dimensional ADI-FDTD method," *IEEE Microwave Guided Wave Lett.*, vol. 10, pp. 261–263, July 2000.
[10] A. P. Zhao, J. Juntunen, and A. V. Raisanen, "Generalized material-independent PML absorbers for the FD-TD simulation of electromagnetic waves in arbitrary anisotropic dielectric and magnetic media," *IEEE Microwave Guided Wave Lett.*, vol. 8, pp. 52–54, Feb. 1998.